

EXPERIMENTAL STUDY ON SLENDER RECTANGULAR RC WALLS (PART I: EXPERIMENTAL PROGRAM)

Slender Wall Flexural Failure Ultimate drift
High Axial Load Fiber Model

○Tatsuya TAKAHASHI*1 Chanipa NETRATTANA*1
Taku OBARA*1 Susumu KONO*1
David MUKAI*2

1 Introduction

Rectangular cross-section reinforced concrete (RC) walls are favored seismic resisting system in mid-rise and high-rise buildings. After the 2010 Chile earthquake [1] and 2011 Christchurch earthquake [2], concerns about flexural failure with concrete crushing and buckling of longitudinal reinforcement in slender RC wall were raised.

This paper presents experimental load-drift relations, failure mode and ultimate drift capacities of four slender RC wall specimens in part I. Simulation of load-drift relations and ultimate drift capacities is presented in part II.

2 Experimental Program

Tested units consisted of four rectangular cross-section cantilever RC walls subjected to quasi-static cyclic loading.

2.1 Specimen Properties

Specimens were RC walls with confined end region. Geometry and reinforcement details are shown in Fig. 1. Specimen properties are summarized in Table 1. All specimens had 900 mm of wall length and 1800 mm of wall height.

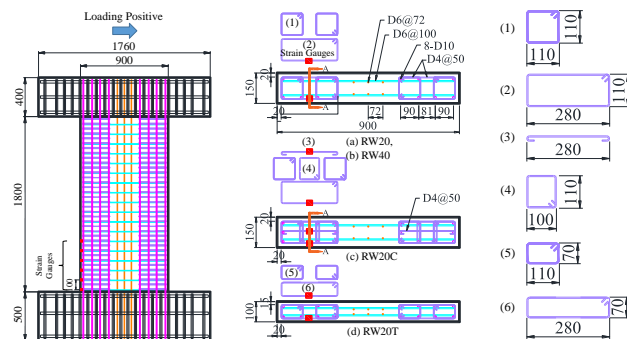


Fig.1 Geometry and reinforcement detail (unit: mm)

Table1 Specimen properties

| Specimen | Major Parameter | tw (mm) | Confined Area | | | | η | $\frac{Q_{su}}{Q_{fu}}$ |
|----------|-----------------|---------|---------------------|--------------|---------------------------|--------------|--------|-------------------------|
| | | | Vert. reinforcement | | Confinement reinforcement | | | |
| | | | Detail | ρ_v (%) | Detail | ρ_s (%) | | |
| RW20 | Bench Mark | 150 | 8D10 | 1.84 | 1.35 | 0.20 | 1.8 | |
| RW20T | Thickness | 100 | | 2.90 | | | 1.77 | 2.2 |
| RW20C | Hoop | 150 | | 1.84 | 2.53 | | 1.8 | |
| RW40 | Axial load | | | 1.35 | 0.40 | | 1.7 | |

t_w : wall thickness, ρ_v : vertical reinforcement area to confined concrete area ratio, ρ_s : confined reinforcement volume to confined concrete volume ratio, η axial load ratio, Vertical reinforcement and horizontal reinforcement in wall panel were 2-D6@72 and 2-D6@100. D4@50a : hoop with tie-bars reinforcement. Flexural load capacity, Q_m , was calculated by cross-section analysis. Shear capacity, Q_{su} , followed ACI 318 [3] equations.

2.2 Material Properties

Table 2 and 3 present mechanical properties of concrete and steel reinforcement.

Table2 Mechanical properties of concrete

| Specimen | Compressive strength (MPa) | Young's modulus (GPa) | Splitting Tensile strength (MPa) |
|----------|----------------------------|-----------------------|----------------------------------|
| RW20 | 34.2 | 22.7 | 2.64 |
| RW20T | 32.0 | 23.0 | 3.60 |
| RW20C | 36.9 | 24.2 | 2.95 |
| RW40 | 38.7 | 27.5 | 3.05 |

Table3 Mechanical properties of reinforcing steel

| Specimen | Rebar | Yield Strength (MPa) | Young's modulus (GPa) | Tensile strength (MPa) |
|-------------|-------|----------------------|-----------------------|------------------------|
| RW20, RW20T | D10 | 351 | 189 | 455 |
| | D6 | 382* | 206 | 529 |
| | D4 | 400* | 187 | 531 |
| RW20C, RW40 | D10 | 357 | 187 | 501 |
| | D6 | 387* | 196 | 546 |
| | D4 | 385* | 189 | 543 |

*Yield strength was determined from 0.2% offset point.

2.3 Test Setup

Axial load was applied with two vertical hydraulic jacks and kept constant throughout testing. Then, horizontal cyclic displacement was applied two cycles at each limit drift. Limit drift comprised of 0.125%, 0.25%, 0.5%, 0.75%, 1%, 1.5%, 2%, 3% and 4%. Specimen was loaded as cantilever with contraflexure point 3000 mm above bottom stub. Shear span to depth ratio was 3.3.

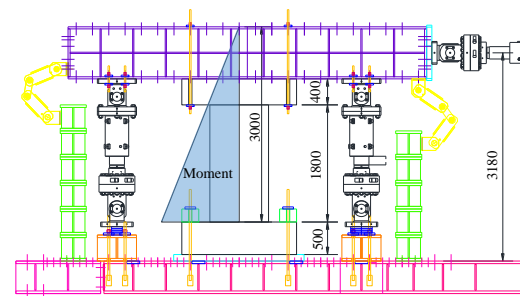


Fig.2 Loading system

3 Failure mode

Figure 3 presents lateral load, Q , and drift, R , relations with four characteristic points. These characteristic points includes flexural cracking, yielding of vertical reinforcement, maximum load and ultimate point.

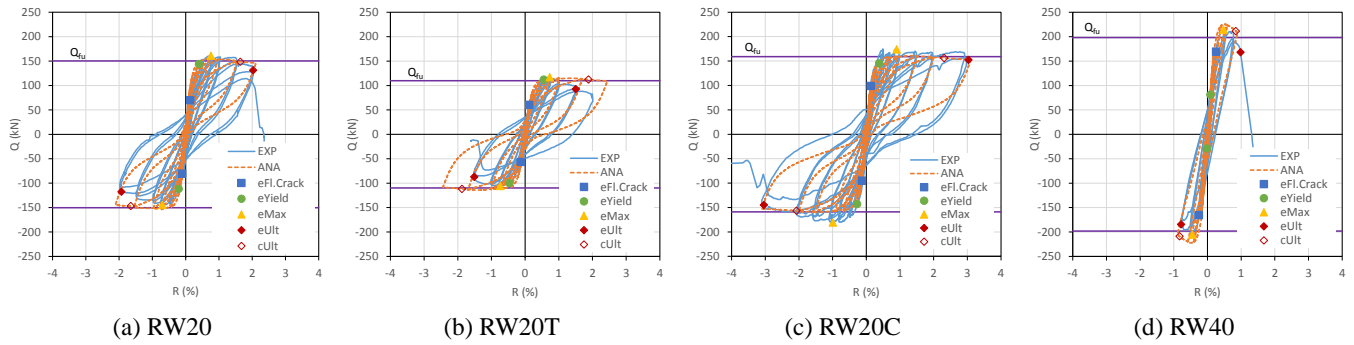


Fig.3 Load-drift relation and characteristic points

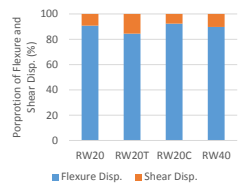


Fig.4 Proportion of flexure and shear displacement at maximum load

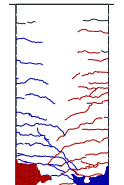


Fig.5 Cracks at R=2.0% of RW20



Fig.6 Concrete crushing along wall length of RW20

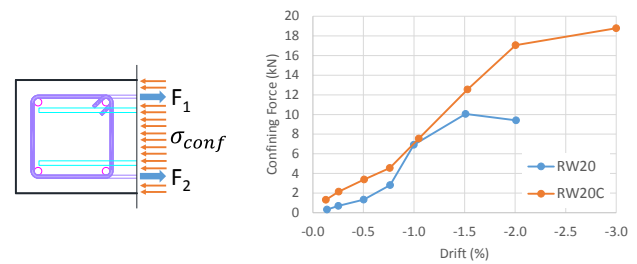


Fig.7 Confining force of RW20 and RW20C

Ultimate point was defined when load drops to 80% of maximum load. Displacement of all specimens was governed by flexural displacement as shown in Fig.4. Figure 5 shows crack pattern at R=2.0% for RW20. Because of large ratio of shear to flexure capacity, large proportion of flexural displacement, and large amount of flexural cracks, four specimens were dominated by flexural behavior.

However, four specimens showed sudden lateral load drop at the end of loading. Concrete crushed along wall length as shown in Fig.6 and brittle out-of-plane movement occurred, and they caused sudden drop of lateral load. Four specimens had a brittle collapse after passing the ultimate point.

Figure 3 shows that degradation of lateral load capacity after maximum load in RW20T was faster than RW20. Stiffness of load degradation path in RW20C was 1.4 times of RW20. Buckling of longitudinal reinforcement was observed visually at R=-1.5% in RW20T and R=1.5% in RW20. Buckling of longitudinal reinforcement, thinner cover concrete than other specimens as shown in Fig.1, and thinner wall thickness might have caused fast load degradation in RW20T. For this reason, ultimate drift capacity of RW20T was reduced from 2.03 % to 1.50% drift.

RW20C with additional confining reinforcement by hoop and tie reinforcement contributed to increased lateral load capacity from 161 kN to 174 kN and increased ultimate drift from 2.03 % to 3.03 %. Stiffness of load degradation path in positive direction of RW20C was 0.4 times of RW20. Figure 7 shows confining force at section A-A in Fig. 1 of RW20 and RW20C.

The confining force calculated from strain of hoop and tie reinforcement. Tensile force in hoop and tie reinforcement balances with confined concrete compressive force ($\sigma_{conf} \times Area$). RW20C had larger confining force than RW20 between R=-1.5% to R=-2.0 %.

Increasing axial load ratio from 20% to 40%, ultimate drift capacity dramatically reduced from 2.03 % to 0.98 %. Ultimate drift capacity of RW40 was determined by the brittle collapse.

4 Conclusions

Flexure mode was dominant behavior until ultimate point and load-drift relations and their ultimate drift capacities can be simulated by with fiber based model in part II.

5 References

- Wallace, J.W., Massone, L.M., Bonelli, P., Dragovich, J., Lagos, R., Lüders, C. and Moehle, J. (2012). Damage and implications for seismic design of RC structural wall buildings. *Earthquake Spectra*, 28(1), 281-299.
- Kam, W.Y., Pampanin, S. and Elwood, K. (2011). Seismic performance of reinforced concrete buildings in the 22 February Christchurch (Lyttelton) earthquake. *Bulletin of the New Zealand Society for Earthquake Engineering*, 44(4), 239-278.
- ACI (American Concrete Institute). (2011). Building code requirements for structural concrete and commentary. ACI 318-11, Detroit.

*1 Tokyo Institute of Technology

*2 University of Wyoming